



HAL
open science

State diagram of whole milk for freeze-drying application

Fadwa Alla, Émilie Gagnière, Géraldine Agusti, Maria Perez Rodriguez,
Anouar Rich, Mohammed Mountadar, Mostapha Siniti, Claudia Cogné

► To cite this version:

Fadwa Alla, Émilie Gagnière, Géraldine Agusti, Maria Perez Rodriguez, Anouar Rich, et al.. State diagram of whole milk for freeze-drying application. *Journal of Crystal Growth*, 2023, 622, pp.127349. 10.1016/j.jcrysro.2023.127349 . hal-04212721

HAL Id: hal-04212721

<https://cnrs.hal.science/hal-04212721>

Submitted on 5 Oct 2023

HAL is a multi-disciplinary open access archive for the deposit and dissemination of scientific research documents, whether they are published or not. The documents may come from teaching and research institutions in France or abroad, or from public or private research centers.

L'archive ouverte pluridisciplinaire **HAL**, est destinée au dépôt et à la diffusion de documents scientifiques de niveau recherche, publiés ou non, émanant des établissements d'enseignement et de recherche français ou étrangers, des laboratoires publics ou privés.

1 State diagram of whole milk for freeze-drying application

2 Fadwa ALLA^{1,2}. Émilie GAGNIERE¹. Géraldine AGUSTI¹. Maria PEREZ RODRIGUEZ, Anouar
3 RICH². Mohammed MOUNTADAR². Mostapha SINITI² and Claudia COGNÉ¹

4 ¹Univ Lyon, Université Claude Bernard Lyon 1, CNRS, LAGEPP UMR 5007, 43 boulevard du 11
5 novembre 1918, F-69100, Villeurbanne, France

6 ²Laboratoire de Chimie de Coordination et d'Analytique (LCCA), Equipe Thermodynamique
7 Appliquée et Procédés (ETAP). Faculté des Sciences El Jadida, Université Chouaib Doukkali, PO Box
8 20, El Jadida, M-24000, Morocco.
9 E-mail: Fadwa.alla95@gmail.com

10 *Abstract*

11 The state diagram is a key parameter when optimizing a freeze-drying cycle, as it allows us to
12 set the optimum processing temperature for a specific product. The purpose of this work is to
13 provide some thermodynamic and physicochemical data for optimizing the freeze-drying
14 cycle of whole milk. **Freezing point measurements were determined using differential
15 scanning calorimetry and cryoscopy methods, and glass transitions were evaluated by DSC.**

16 The endothermic peak was used as the equilibrium freezing point, a variation from 273.93 K
17 to 264.92 K was detected when the dry matter content varied from 0 to 75%. T_g midpoint
18 temperature was used as glass transition of dry mater. Furthermore, Fox and Gordon-Taylor
19 equations were used to predict the glass transition curve to determine T_g' , this temperature
20 was used as an approximation of the critical temperature T_c . Collapse temperature was
21 determined using the freeze-drying microscopy setup.

22 **Key words:** A1. State diagrams, A1. Characterization, A1. Solidification, A1. Optical
23 microscopy, A1. Freeze-drying

24 *1. Introduction*

25 Milk is a complex mixture of ingredients. Liquid water, arguably the most important solvent
26 on Earth, is the main component of whole milk representing more than 86% of the total mass
27 of cow milk. The most important compounds in milk are lactose, fat and protein. Dry food is

28 thus much more stable than wet food. Water in dairy products contributes to microorganisms
29 growth and acts as a plasticizer for non-fat (carbohydrates and proteins) milk solids [1]. One
30 process that can be used to promote the long-term stability of these products while avoiding
31 thermal degradation of their structure is freeze-drying (also known as lyophilization).

32 Freeze-drying is a low-temperature, low-pressure dehydration process that is time-consuming
33 and energy-intensive. It consists of three main steps: freezing, primary drying and secondary
34 drying. In the first step, the product can be frozen at an extremely low temperature around
35 -60°C and most of the water solvent is converted to ice. In the second step, the ice is removed
36 from the frozen product by sublimation [2], **the primary drying must be performed at a**
37 **temperature below collapse point T_c (i.e. maximum allowable product temperature during**
38 **primary drying for an amorphous system).** In the final step, the unfrozen water that has not
39 crystallized during freezing and is bound to the product is desorbed at a higher temperature
40 [3]. Primary drying is the most time and energy consuming step in the entire process [4].

41 Therefore, the optimization of this step is of paramount importance to accelerate the
42 development of freeze-drying process. It is well known that increasing the temperature will
43 significantly increase yield during sublimation [5][6]. Indeed, a temperature increase of only
44 1°C resulted in a reduction of at least 13% in primary drying time [5][7]. Thus, **to optimize**
45 **the freeze-drying cycles it is necessary to determine the key parameters i.e. T_g , T_g' and T_c .** T_g
46 can be defined as the temperature at which an amorphous system changes from glassy to
47 rubbery. It has been used as an indicator of food stability and to predict food behavior,
48 whereas for a concentrated solution at the freezing maximum, the notation is T_g' [8], Glass
49 transition temperature (T_g) of any milk powder, is primarily the effect of amorphous lactose,
50 the amorphous lactose coats milk proteins and fat globules in a glassy powder [9]. The
51 collapse temperature T_c is related to the glass transition temperature T_g' but is not the same the
52 latter being slightly lower even when measured at low rates [5] T_c is usually determined by

53 freeze-drying microscopy (FDM) while the standard method for T_g' is Differential Scanning
54 Calorimetry (DSC) [10][11]. Small molecules act as plasticizers when mixed with larger
55 molecules by lowering the apparent glass transition temperature of the latter [9]. The most
56 common plasticizer in the food industry is water. As suggested in the literature, the glass
57 transition temperature T_g' can be used as a first approximation of the collapse temperature. The
58 T_g of skimmed milk powder is easier to determine than whole milk powder (WMP). The glass
59 transition temperature of WMP is dependent on the water content, which overlaps more or
60 less with the end point of fat melting in a given water content [9]. To fully understand what
61 occurs in freeze drying, it is also necessary to consider the role of ice formation, both
62 processes are best understood with reference to a state diagram.

63 State diagram is a tool for optimizing the drying process because it depicts the different states
64 of the food, describes equilibria such as freezing point and glass transition, which helps to
65 understand the complex changes that occur when the water content of a food is modified. It
66 also helps to identify the stability of food during storage and to select the appropriate
67 temperature and moisture content [9]. In order to establish the solid-liquid equilibrium
68 temperature of a mixture, the commonly used methods are cryoscopy and DSC. AOAC
69 (Association of Official Analytical Chemists) usually uses the cryoscopy method to quantify
70 adulteration of milk with water, the solution is cooled until solidification, the temperature-
71 time is observed with a temperature-indicator, and initial or equilibrium freezing point is used
72 as the maximum temperature after ice nucleation (e.i plateau) [12]. While cryoscopy has been
73 shown to be effective, it requires manual observation and often does not provide information
74 on other thermodynamic properties of interest. The amount of solute must be negligible
75 compared to the amount of solvent in a liquid solution [13]. In addition, serious complications
76 can arise from operating cryo-devices at low temperatures. The application of DSC to the
77 study of organic mixtures has shown the development of several methods for the

78 determination of the liquidus temperature (T_{liquidus}) from the thermogram observed during the
79 melting of the solid phase [14]. The freezing point is usually characterized from the
80 endothermic peak during the melting process [15]. The freezing point could be considered as
81 the temperature peak or at the onset point of the endothermic peak [15], although the melting
82 point in mixtures are qualitatively different from those in pure substances. The use of a low
83 heating rate is important to ensure a steady state during heating. It is important to note that the
84 freezing point of water and other liquids can be at the same temperature as the melting point.
85 It won't be higher, but it could easily be lower.

86 The objective of this study is to realize the state diagram of whole milk by measuring glass
87 transition temperature and freezing curves to find the maximal-freeze-concentration
88 condition, in order to better understand the freeze-drying applied effect. This was possible by
89 using a low-cost and simple cooling curve method (cryoscopy) to measure the freezing point
90 T_f and to compare with DSC results obtained from the melting curve.

91 **2. Experimental Methods.**

92 **2.1. Samples preparation.**

93 To plot the state diagram of the water/WMP mixture, samples with different dry matter were
94 prepared using the same brand of milk powder “Commercial name Nido”, with initial
95 moisture content of 3% dry matter (measured using Karl Fisher apparatus). **Tab.1** presents the
96 main information about this product. The concentrations of the solutions were calculated
97 using **Eq1**.

$$98 \quad W_{p.w} = \frac{m_p}{m_p + m_w} \quad \text{Eq.1}$$

99 Where $W_{p.w}$ is the weight concentration of the solution, m_p is the mass of Milk powder and
100 m_w is the mass of distilled water.

101 To complete the discussion about the collapse temperature, some analysis have been done on
102 liquid whole milk, (noted WM) that contains 12.4% of dried matter with (3.6g for 100ml of
103 fat content).

104 *2.2. State diagram of whole milk*

105 *2.2.1. Cryoscopy “cooling curve”*

106 Freezing point depression (FPD) is one of the most important thermophysical properties of an
107 aqueous solution for freezing processes [13]. *Fig.1* shows the experimental setup used to
108 determine the solid/liquid equilibrium of milk solutions. The cryoscopy apparatus used in this
109 study is from PHYWE, it consists of two cylindrical DURANglass vessels (1-3). One fits into
110 the other and is secured by a screw cap GL 45. The inner cylindrical glass vessel has a
111 capacity of 60 ml with a flat bottom to accommodate a magnetic stirring bar and a side inlet
112 for the introduction of the product. The outer jacket glass is filled with 35-40 ml of ethanol to
113 ensure a uniform heat transport from the inner vessel to the frozen mixture. The set of two
114 cylindrical tubes was immersed in a 1000 ml glass beaker filled with a suitable freezing
115 mixture of crushed ice and sodium chloride to achieve a temperature near to -22 °C. The
116 whole equipment is placed under stirring using magnetic stirrer. The temperatures in the inner
117 cylindrical glass vessel and cooling bath are measured by two Pt100 immersion temperature
118 probes (5) connected to the data acquisition system (6).

119 The solutions were cooled at a cooling rate of approximately 1.6 °C/min. The experimental
120 study of the solid-liquid equilibrium was carried out for milk solution at concentrations of dry
121 matter ranging from 0 wt % to 50 wt % dry matter. Aqueous solutions were prepared using
122 sucrose as analytical reagent, varied from to 273.15 to 263.39 K when solids content changed
123 from 0 to 49.5%. The FPD of this solution is available in literature, allowing the comparison
124 of our results and the literature data. To further confirm the measurement procedure in the

125 high concentration range [13]. Equilibrium points are synthesized from a temperature plateau
126 (temperature-time curve) over a long period as shown by *Fig.2*.

127 *2.2.2. Calorimetric Analysis by Differential Scanning Calorimetry*

128 Freezing point and glass transition of whole milk sample at different dry matter content were
129 measured by DSC. The Differential Scanning Calorimetry instrument used was a TA
130 Instruments DSC Q200 with Universal Analysis Software, to determine the state transition
131 temperatures. Milk solution samples (20-25 mg) from 0% (wt) to 75% (wt) dry matter were
132 prepared, each sample was pipetted into a DSC pan and weighed with a Mettler balance to an
133 accuracy of 0.01 mg. Hermetically sealable aluminum sample pans were used in all
134 measurements with an empty aluminum pan as a reference, equilibrated at 20°C. Afterward,
135 the temperature was decreased to -40°C and then increased to 40°C at a rate of 1°C min⁻¹, two
136 scans were performed for each sample. All measurements were performed under a nitrogen
137 atmosphere with a flow rate of 50 mL min⁻¹ used to purge the sample head for all
138 measurements to avoid condensation in the oven. The results reported in this work correspond
139 to data as a function of temperature, with the freezing temperature acquired at the peak of the
140 melting of the heat flow curve at the second melting scan. Fig.3 represents an example of
141 DSC thermogram of whole milk sample containing 20% dry matter.

142 *2.2.3. Freeze-drying microscopy (FDM)*

143 Linkam Scientific FDCS196 freeze drying cryo-stage and optical microscopy LEICA (DM)
144 were used to observe the behavior of the solutions during both cooling and warming periods.
145 A microscope slide made of quartz (16-mm) and oil was used to enhance thermal contact
146 between the sample and the temperature-controlled plate. A drop of 2-3 µl of sample (10wt%,
147 12.4wt% and 20wt% of WMP and commercial WM) was prepared. A second slide was gently
148 pressed on top to form a seal tight enough to prevent sample water from evaporating, the

149 samples were then transferred into the microscope chamber. A Sony CCD camera with 1600 x
150 1200 pixels was used to record pictures.

151 **3. Results and discussion**

152 **3.1. Experimental Solid–Liquid state Diagram: Freezing point**

153 Whole milk state diagram has been studied to identify the phase transitions that can occur at a
154 specific temperature and weight fraction. Experimental state diagram was investigated using
155 two methods: Cryoscopy and DSC analysis to determine freezing point. Whole milk samples
156 were prepared by diluting concentrated milk with distilled water. Cryoscopy method was used
157 for milk solutions with concentrations ranging from 0 to 50% dry mater and the DSC analysis
158 was used for milk solutions with concentrations ranging from 0 to 75% dry matter. According
159 to literature [13], freezing points can be derived from long temperature plateau when
160 cryoscopy method is used, it can be also determined from melting peak at the endothermic
161 curve using DSC [15].

162 **Fig.4** represents the melting curves obtained using DSC at a heating rate of $1^{\circ}\text{C}\cdot\text{min}^{-1}$ for
163 different dry matter contents. When the heating rate decreases and approaches zero, the
164 temperature gradient within the sample decreases [16], that is why a low heating rate was
165 applied. Freezing point results are summarized in **Tab.2**.

166 According to literature work, it is more reasonable to consider the maximum of the
167 endothermic peak as the freezing point to develop the state diagram using DSC, in the case of
168 food products [15][17][18][19].

169 Chen et. al [13] results were used to compare the liquidus temperatures measured by the
170 cryoscopy and DSC as shown in **Fig.5**. Both methods showed good consistency, increasing
171 amount of milk powder leads to a decreasing of freezing point. However, the equilibrium
172 temperatures given by the synthetic method tends to be lower at certain points than the

173 temperatures obtained by DSC. For fact that the freezing point of a substance largely depends
174 on supercooling, while supercooling has no effect on the melting point of a substance.
175 Cryoscopy results [13] have been used to determine the freezing point to build the model state
176 diagram of whole milk [9].

177 However the reliability of cryoscopy results lies in the study of solutions with low solute
178 concentration [13], the cooling curve lost its sensitivity at high dry matter content, due to the
179 low amount of freezable water present in the sample. We find out that using DSC for the
180 construction of equilibrium state diagrams is becoming common; the advantages of DSC lies
181 in its speed of measurement and ease of use. It has been widely used in the study of protein
182 denaturation, carbohydrate stability, and the determination of first and second-order
183 transitions in lipids [20] [21][22]. **Based on all of that, the DSC results seem to be more**
184 **accurate than cryoscopy method in our case.**

185 **3.2. Glass transition**

186 The study of the effect of heating rates on glass transition T_g was performed using a
187 commercial whole milk powder containing 3 % water content **Fig. 6** shows the graphical
188 results of T_g at different heating rates (1; 5; 10 and 20 °C/min). Heating rate was found to
189 have an effect on the T_g value, with a significant decrease in the glass transition from 65.55 to
190 54.15 °C when the scanning rate was reduced from 20 to 1°C/min, the use of a low heating
191 rate is important to ensure a steady state during heating. Therefore, the lowest heating rate
192 was selected for the T_g measurements. Glass transition was difficult to detect for WMP
193 between 4 and 8.5 % water content, as reported in the literature [9]. In addition, it was not
194 possible to determine T_g from the DSC curves of fat-containing with a water content range of
195 23.9 to 44.4 % because the fat-melting endothermic predominates in the same temperature
196 range [23] **Tab. 3** shows the T_g results of weight mass fraction (93.3 and 97%) for whole milk

197 powders at a heating rate of 1 °C/min. The glass transitions are reported as the midpoint
198 temperatures: the glass-transition mid-point value was obtained as an average of the onset and
199 end values [24], the glass transition temperature increased as solid content increased.

200 Glass transition of mixtures can be predicted using various empirical equations. The reliability
201 of T_g depends on the accuracy of the determination of total solids in milk. In this paper, the
202 Gordon-Taylor and Fox equations were established to predict the T_g curve of amorphous
203 whole milk, considering that all solid components which contributing to the observed glass
204 transition were miscible and formed a single phase. The Gordon-Taylor equation seems to be
205 most commonly applied to amorphous foods to describe the plasticity of solids by water
206 [9][25].

$$207 \quad T_{g,m} = \frac{W_1 T_{g,1} + K(1 - W_1) T_{g,2}}{W_1 + K(1 - W_1)} \quad Eq.2$$

208 Where W_1 and W_2 are the weight fractions of solute and water, respectively. The model
209 requires knowledge of three constants: the coefficient K, which represents the non-linearity of
210 plasticizing effect of water. $T_{g,1}$ is the T_g of anhydrous solute and $T_{g,2}$ is the T_g of water.
211 However, it is difficult to dehydrate amorphous food powders by heating without significant
212 chemical changes, recrystallization or structural changes. That is why we used the literature as
213 defining parameters for our datasets: $T_{g,1} = 373.75$ K, $K = 8.57$ [9] ($T_{g,1}$ is close to T_g of pure
214 lactose [23][26][27]), and $T_{g,2} = 138$ K (glass transition temperature for pure water) [15][28].
215 The T_g curve with Gordon-Taylor equation for whole milk is presented on **Fig. 7** (Orange
216 curve). A predicted glass transition curve is also obtained using the Fox equation (Eq.3) for
217 approximate estimation of T_g of binary system [29].

$$218 \quad \frac{1}{T_{g,m}} = \frac{W_1}{T_{g,1}} + \frac{W_2}{T_{g,2}} \quad Eq.3$$

219 Where the definition of W_1 , W_2 , $T_{g,1}$, and $T_{g,2}$ is the same as **Eq.2**. As mentioned earlier, it is
220 difficult to measure the T_g of anhydrous milk. In this section, we predicted the $T_{g,1}$ using the
221 $T_{g,m}$ of 97 % dry matter of the commercial powder. The T_g curve of the Fox equation is
222 shown in **Fig.7** (blue curve). The most accurate model to build glass transition curve for our
223 state diagram seems to be Gordon-Taylor equation.

224 T_g' is defined as the intersection of the freezing curve with the glass line. The T_g' corresponds
225 to the glass transition of the matrix (mixture of dry matter and unfrozen water) in the frozen
226 sample. It is an important process parameter during freeze-drying. The T_g' is approximately
227 read between -48°C and -23°C , corresponding to a maximally freeze-concentrated solution
228 read between 83% and 88 % of WMP using Gordon-Taylor curve (**Fig.7,**) result closed to
229 what has already been found by the authors [23]. **The T_g' of lactose in food are respectively -**
230 **41°C and -28°C for 0.813 and 0.592g dry solid/g food [30][19].** This prediction is important
231 to determinate the collapse temperature (T_c) currently assimilated to the T_g' as a first
232 approximation.

233 **3.3. Collapse temperature**

234 The collapse temperature (T_c) of whole milk is measured by direct microscopic observation
235 under simulated low-temperature, low-pressure freeze-drying conditions. Samples containing
236 in weight 10%, -12.4%, 20% WMP and a commercial WM with 12.4% were selected for
237 Freeze-drying microscopic observation of the physical state of the WMP/water system. The
238 sample was frozen to a temperature lower than T_g' (about -50°C) below the lowest
239 temperature value in the T_g' range. Then, the sample was kept at this temperature for 1 min,
240 then the system was placed under vacuum at about 10 Pa (operating limit of our freeze dryer
241 during sublimation). The temperature was increased by $10^\circ\text{C}/\text{min}$ until -40°C . **At -40°C , we**
242 **noted that samples were not collapsed (Fig 8). Then the temperature is gradually increased at**

243 0.5°C/min until a collapse was observed up to -36°C, -37°C, -38°C and -35°C respectively for
244 solution 10%, 12.4%, 20% of WMP and WM with 12.4% (**Fig 9**), the collapse temperature
245 (T_c) is observed by the formation of micro-cracks during the displacement of a front between
246 two zones, a frozen zone and a dried zone as shown in **Fig. 9**.

247 We can conclude that the T_c is slightly depending on the WMP amount content of the initial
248 solution of whole milk. This collapse temperature value is in adequation with the T_g' ,
249 currently T_c is often reported to be higher (1–22°C) than the corresponding T_g' . In last
250 decades, the T_g' has mainly been used as the critical temperature, collapse temperature is now
251 known to better reflect drying conditions [25][31][27] [7].

252 *Conclusion*

253 In this work, DSC data were used to design the solid/liquid state diagram of the water/WMP
254 system with the peak of the endothermic curve as the freezing point and the midpoint as the
255 glass transition temperature. The freezing points of whole milk were varied from to 273.93 to
256 269.55 K when dry matter content changed from 0 to 75% using DSC, respectively. DSC
257 results were consolidated using cryoscopy experimental data. These data allow us to calculate
258 the glass transition evolution versus mass fraction of WPM using two models, Fox and
259 Gordon-Taylor equations. In addition, the collapse temperature has been evaluated by Freeze-
260 drying microscopy.

261 These new experimental data concerning whole milk allow us to fix the critical temperatures
262 of freeze-drying cycles of milk formulations in order to optimize the process time and the
263 energy consumption.

264 *Acknowledgment*

265 This study was supported by the Franco-Moroccan Interuniversity Committee, Hubert Curien
266 / Toubkal program, the authors are grateful to the Campus France program for the financial
267 support received during this work “*Number: Toubkal/21/125 - Campus France: 45806RC*”

268 *References*

- 269 [1] O. Fox, P.F., Uniacke-Lowe, T., McSweeney, P.L.H., “Water in Milk and Dairy Products. In:
270 Dairy Chemistry and Biochemistry,” *Springer, Cham*, 2015, [Online]. Available:
271 https://doi.org/10.1007/978-3-319-14892-2_7
- 272 [2] Y. H. Roos, “Glass transition temperature and its relevance in food processing,” *Annu. Rev.*
273 *Food Sci. Technol.*, vol. 1, no. 1, pp. 469–496, 2010, doi:
274 10.1146/annurev.food.102308.124139.
- 275 [3] C. T. and M. J. Pikal, “Design of Freeze-Drying Processes for Pharmaceuticals: Practical
276 Advice,” *Pharm. Res.*, vol. 34, no. October 2004, 2004, doi:
277 0.1023/B:PHAM.0000016234.73023.75B.
- 278 [4] L. Stratta, L. C. Capozzi, S. Franzino, and R. Pisano, “Economic analysis of a freeze-drying
279 cycle,” *Processes*, vol. 8, no. 11, pp. 1–17, 2020, doi: 10.3390/pr8111399.
- 280 [5] M. J. Pikal and S. Shah, “The collapse temperature in freeze drying: Dependence on
281 measurement methodology and rate of water removal from the glassy phase,” *Int. J. Pharm.*,
282 vol. 62, no. 2–3, pp. 165–186, 1990, doi: 10.1016/0378-5173(90)90231-R.
- 283 [6] G. Bano, R. De-Luca, E. Tomba, A. Marcelli, F. Bezzo, and M. Barolo, “Primary Drying
284 Optimization in Pharmaceutical Freeze-Drying: A Multivial Stochastic Modeling Framework,”
285 *Ind. Eng. Chem. Res.*, vol. 59, no. 11, pp. 5056–5071, 2020, doi: 10.1021/acs.iecr.9b06402.
- 286 [7] J. Horn and W. Friess, “Detection of collapse and crystallization of saccharide, protein, and
287 mannitol formulations by optical fibers in lyophilization,” *Front. Chem.*, vol. 6, no. JAN, pp.
288 1–9, 2018, doi: 10.3389/fchem.2018.00004.
- 289 [8] S. K. Pansare and S. M. Patel, “Practical Considerations for Determination of Glass Transition
290 Temperature of a Maximally Freeze Concentrated Solution,” *AAPS PharmSciTech*, vol. 17, no.
291 4, pp. 805–819, 2016, doi: 10.1208/s12249-016-0551-x.

- 292 [9] G. Vuataz, "The phase diagram of milk: A new tool for optimising the drying process," *Lait*,
293 vol. 82(4), pp. 485–500., 2002, doi: <https://doi.org/10.1051/lait:2002026>.
- 294 [10] F. Fonseca, S. Passot, P. Lieben, and M. Marin, "Collapse temperature of bacterial
295 suspensions: The effect of cell type and concentration," *Cryo-Letters*, vol. 25, no. 6, pp. 425–
296 434, 2004.
- 297 [11] P. Verlhac, C. Cogné, S. Vessot, G. Degobert, and J. Andrieu, "Thermodynamic Properties and
298 Water States in Ternary PVP/Lactose/Water Frozen Systems," *J. Chem. Eng. Data*, vol. 63, no.
299 11, pp. 4166–4175, 2018, doi: 10.1021/acs.jced.8b00613.
- 300 [12] M. S. Rahman, N. Guizani, M. Al-Khaseibi, S. Ali Al-Hinai, S. S. Al-Maskri, and K. Al-
301 Hamhami, "Analysis of cooling curve to determine the end point of freezing," *Food*
302 *Hydrocoll.*, vol. 16, no. 6, pp. 653–659, 2002, doi: 10.1016/S0268-005X(02)00031-0.
- 303 [13] P. Chen, X. D. Chen, and K. W. Free, "Measurement and data interpretation of the freezing
304 point depression of milks," *J. Food Eng.*, vol. 30, no. 1–2, pp. 239–253, 1996, doi:
305 10.1016/s0260-8774(96)00047-7.
- 306 [14] S. Gibout, E. Franquet, D. Haillet, J. P. Bédécarrats, and J. P. Dumas, "Challenges of the usual
307 graphical methods used to characterize Phase Change Materials by Differential Scanning
308 Calorimetry," *Appl. Sci.*, vol. 8, no. 1, pp. 1–41, 2018, doi: 10.3390/app8010066.
- 309 [15] M. S. Rahman, "State diagram of date flesh using differential scanning calorimetry (DSC),"
310 *Int. J. Food Prop.*, vol. 7, no. 3, pp. 407–428, 2004, doi: 10.1081/JFP-200032930.
- 311 [16] J. H. Oakley, T. J. Hughes, B. F. Graham, K. N. Marsh, and E. F. May, "Determination of
312 melting temperatures in hydrocarbon mixtures by differential scanning calorimetry," *J. Chem.*
313 *Thermodyn.*, vol. 108, pp. 59–70, 2017, doi: 10.1016/j.jct.2016.12.030.
- 314 [17] Y. - L CHEN and B. S. PAN, "Freezing tilapia by airblast and liquid nitrogen – freezing point
315 and freezing rate," *Int. J. Food Sci. Technol.*, vol. 30, no. 2, pp. 167–173, 1995, doi:
316 10.1111/j.1365-2621.1995.tb01368.x.
- 317 [18] D. Q. WANG and E. KOLBE, "Thermal Properties of Surimi Analyzed using DSC," *J. Food*
318 *Sci.*, vol. 56, no. 2, pp. 302–308, 1991, doi: 10.1111/j.1365-2621.1991.tb05267.x.
- 319 [19] S. S. Sablani, R. M. Syamaladevi, and B. G. Swanson, "A review of methods, data and

- 320 applications of state diagrams of food systems,” *Food Eng. Rev.*, vol. 2, no. 3, pp. 168–203,
321 2010, doi: 10.1007/s12393-010-9020-6.
- 322 [20] A. Pugliese, M. Paciulli, E. Chiavaro, and G. Mucchetti, “Application of differential scanning
323 calorimetry to freeze-dried milk and milk fractions,” *J. Therm. Anal. Calorim.*, vol. 137, no. 2,
324 pp. 703–709, 2019, doi: 10.1007/s10973-018-7971-7.
- 325 [21] M. Siniti, S. Jabrane, and J. M. Létoffé, “Study of the respective binary phase diagrams of
326 sorbitol with mannitol, maltitol and water,” *Thermochim. Acta*, vol. 325, no. 2, pp. 171–180,
327 1999, doi: 10.1016/S0040-6031(98)00576-0.
- 328 [22] J. Tomaszewska-Gras, “Melting and crystallization DSC profiles of milk fat depending on
329 selected factors,” *J. Therm. Anal. Calorim.*, vol. 113, no. 1, pp. 199–208, 2013, doi:
330 10.1007/s10973-013-3087-2.
- 331 [23] K. Jouppila and Y. H. Roos, “Glass Transitions and Crystallization in Milk Powders,” *J. Dairy*
332 *Sci.*, vol. 77, no. 10, pp. 2907–2915, 1994, doi: 10.3168/jds.S0022-0302(94)77231-3.
- 333 [24] M. B. Braga, S. C. dos S. Rocha, and M. D. Hubinger, “Spray-Drying of Milk–Blackberry Pulp
334 Mixture: Effect of Carrier Agent on the Physical Properties of Powder, Water Sorption, and
335 Glass Transition Temperature,” *J. Food Sci.*, vol. 83, no. 6, pp. 1650–1659, 2018, doi:
336 10.1111/1750-3841.14187.
- 337 [25] L. Ozmen and T. A. G. Langrish, “Comparison of glass transition temperature and sticky point
338 temperature for skim milk powder,” *Dry. Technol.*, vol. 20, no. 6, pp. 1177–1192, 2002, doi:
339 10.1081/DRT-120004046.
- 340 [26] K. Jouppila and Y. H. Roos, “Water Sorption and Time-Dependent Phenomena of Milk
341 Powders,” *J. Dairy Sci.*, vol. 77, no. 7, pp. 1798–1808, 1994, doi: 10.3168/jds.S0022-
342 0302(94)77121-6.
- 343 [27] M. E. C. Thomas, J. Scher, S. Desobry-Banon, and S. Desobry, “Milk powders ageing: Effect
344 on physical and functional properties,” *Crit. Rev. Food Sci. Nutr.*, vol. 44, no. 5, pp. 297–322,
345 2004, doi: 10.1080/10408690490464041.
- 346 [28] Y. H. Roos, “Water in Milk Products,” in *Advanced Dairy Chemistry Volume 3*, vol. 3, 1997,
347 pp. 303–346. doi: 10.1007/978-1-4757-4409-5_8.

- 348 [29] W. Brostow, R. Chiu, I. M. Kalogeras, and A. Vassilikou-Dova, "Prediction of glass transition
349 temperatures: Binary blends and copolymers," *Mater. Lett.*, vol. 62, no. 17–18, pp. 3152–3155,
350 2008, doi: 10.1016/j.matlet.2008.02.008.
- 351 [30] Y. Roos, "ScienceDirect.com - Carbohydrate Research - Melting and glass transitions of low
352 molecular weight carbohydrates," *Carbohydr. Res.*, vol. 238, pp. 39–48, 1993, [Online].
353 Available:
354 [http://www.sciencedirect.com/science/article/pii/000862159387004C%5Cnpapers2://publication/](http://www.sciencedirect.com/science/article/pii/000862159387004C%5Cnpapers2://publication/uuid/F2F3CE37-AC6E-470B-9416-9940080A6584)
355 [n/uuid/F2F3CE37-AC6E-470B-9416-9940080A6584](http://www.sciencedirect.com/science/article/pii/000862159387004C%5Cnpapers2://publication/uuid/F2F3CE37-AC6E-470B-9416-9940080A6584)
- 356 [31] D. Champion, M. Le Meste, and D. Simatos, "Towards an improved understanding of glass
357 transition and relaxations in foods: Molecular mobility in the glass transition range," *Trends*
358 *Food Sci. Technol.*, vol. 11, no. 2, pp. 41–55, 2000, doi: 10.1016/S0924-2244(00)00047-9.
- 359
360
361
362
363
364
365
366
367
368
369
370
371
372
373
374
375

376
377
378
379
380
381
382
383
384
385
386
387
388
389
390
391
392
393
394
395
396
397
398
399
400
401
402
403
404
405
406
407

Table 1. Main dry matter components of whole milk powder

<i>Nutrition</i>	<i>WMP per 100 g</i>
Protein	25.7 g
Carbohydrates	36.5 g
Lipids	28.2 g
Salt	0.9 g

408
409
410
411
412
413

Table 2. Experimental results of cryoscopy and DSC^a measurement in our laboratory

$W_{P.M}$ (wt%)	T_f (K)	$W_{P.M}$ (wt%)^a	T_{onset} (K)	T_{peak} (K)
0	273.15	0	271.92	273.93
2.6	273.05	7	270.88	273.53
2.8	273.03	12	270.35	273.06
3.5	273	20	269.4	272.23
4.0	272.98	25	268.79	271.76
4.9	272.95	30	268.18	271.33
6.5	272.88	35	267.42	270.65
7.2	272.85	40	266.7	270
8.2	272.81	45	266.2	269.76
9.3	272.65	50	266.17	269.55
11.4	272.55	60	265.44	269.05
13.3	272.45	70	262.36	267.2
21.6	272.15	75	258.83	264.92
30	271.45			
34.6	270.83			
39.6	270.21			
42.9	269.82			
44.6	269.47			
49.4	268.63			

414 ^a Standard uncertainties (u) are $u_r(\text{wPA}) = 0.001$, $u(T_{\text{eq}}) = u(T_{\text{eut}}) = 1$ K, and $u(P) = 10$ hPa,

415
416
417
418
419
420
421

422

423

424

425

426

427

428

429

430

Table 3: Analytical results for whole milk powder

Mass fraction %	Glass transition K
93.3	304.53
97	327.59

431

432

433

434

435

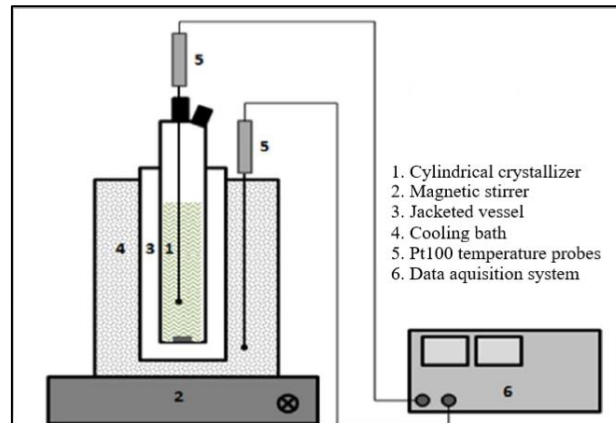
436

437

438

439

440



441

442 *Figure 1. Experimental setup used for the study of the solid-liquid equilibrium.*

443

444

445

446

447

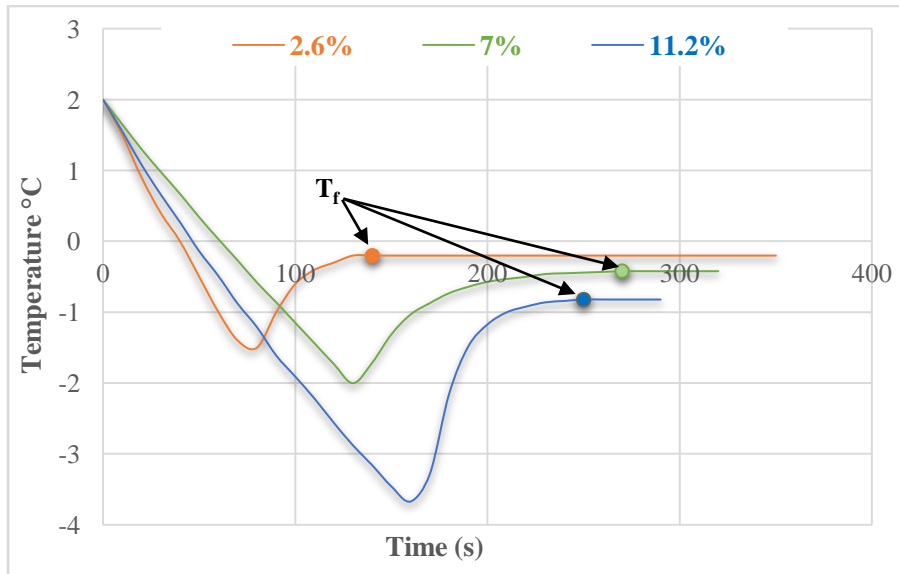
448

449

450

451

452



453

454 *Figure 2. Freezing temperature for whole milk solutions with 6%; 7% and 11.2% (wt) dry*

455 *matter determined from temperature plateau after nucleation.*

456

457

458

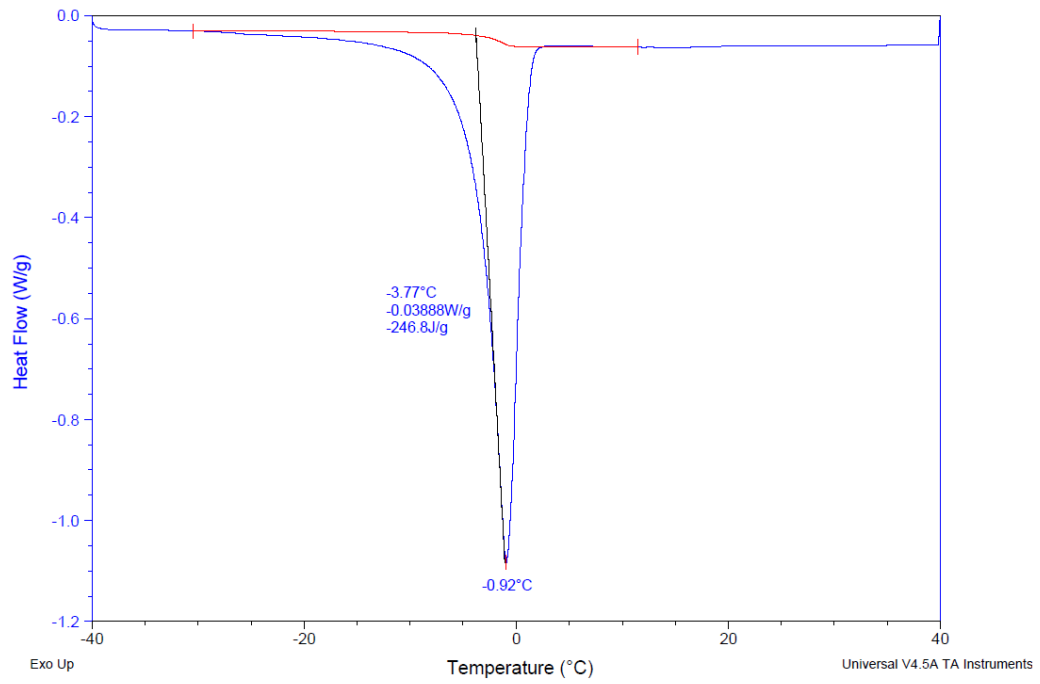
459

460

461

462

463



464

465 *Figure 3. DSC thermogram of whole milk sample containing 20% dry matter.*

466

467

468

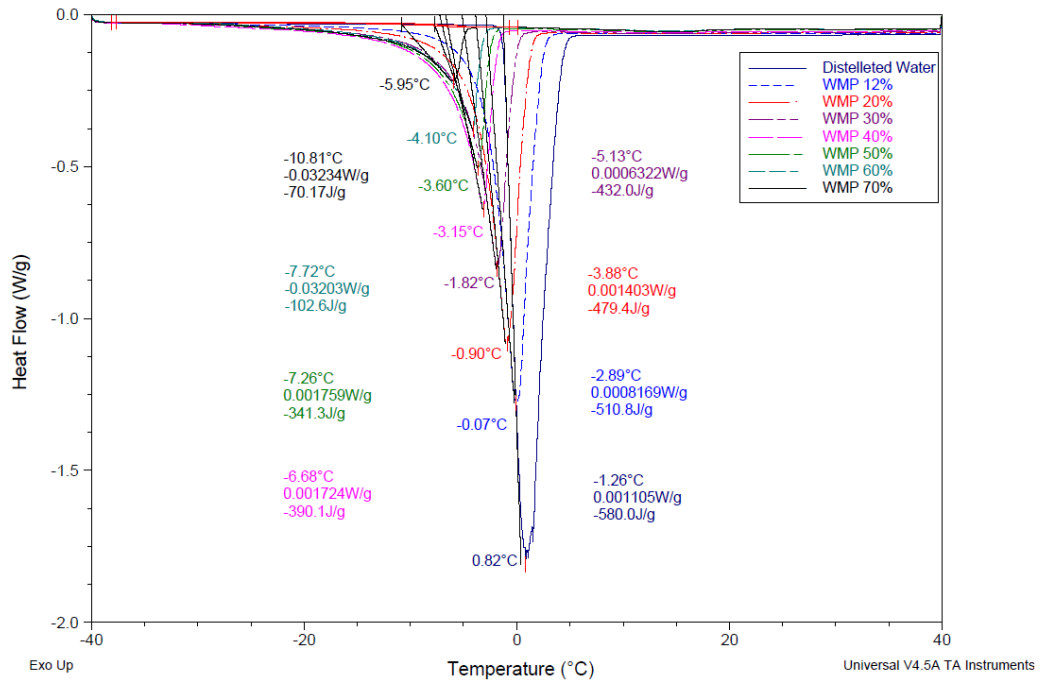
469

470

471

472

473



474

475 **Figure 4.** DSC thermogram of whole milk samples with solids containing 0 to 70% in the 2nd
 476 melting cycle showing the onset and peak temperature of each sample.

477

478

479

480

481

482

483

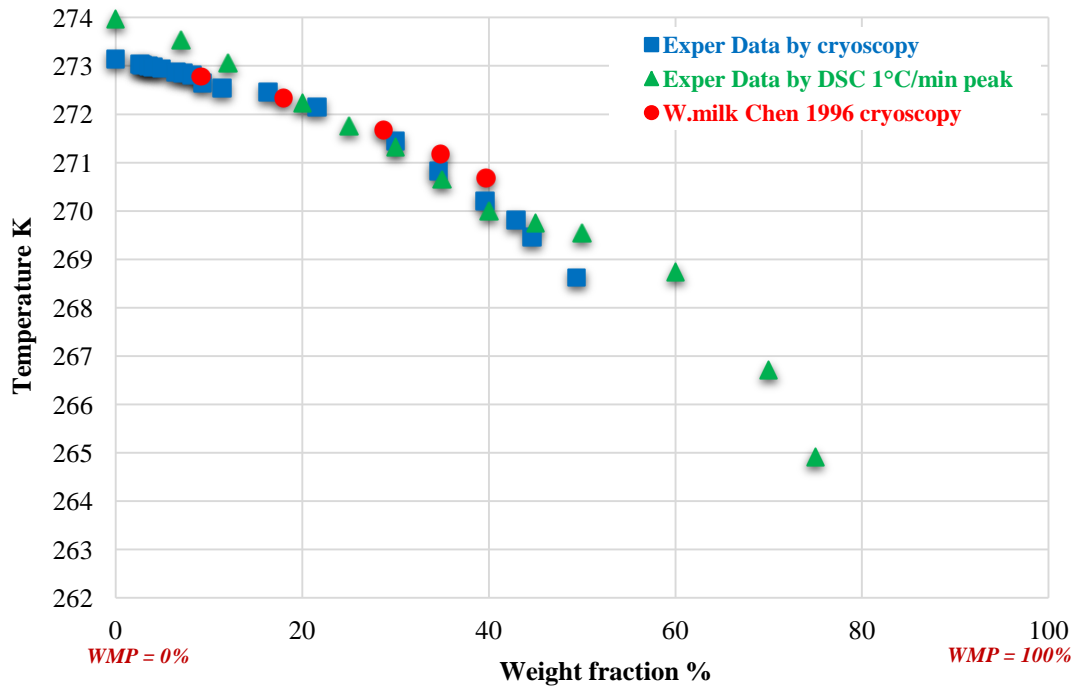
484

485

486

487

488



489

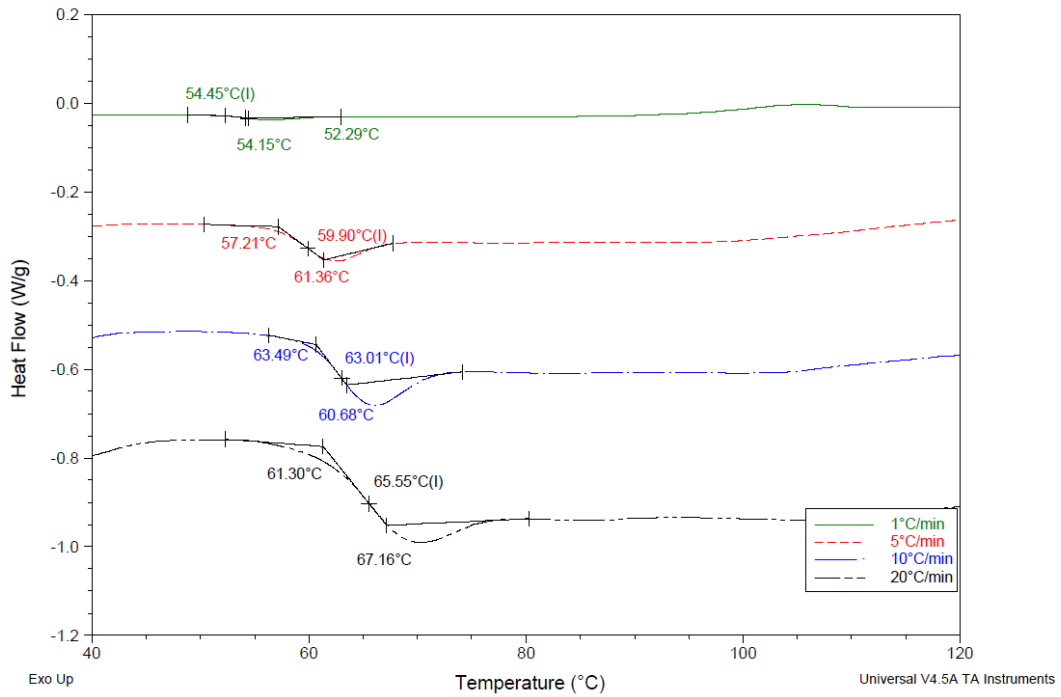
490 *Figure 5. Solid-liquid state diagram of whole milk powder (WMP) using DSC results (green*
 491 *triangle), cryoscopy data (blue square) and Chen et al results (red circle) [12].*

492

493

494

495



496

497

Figure 6. DSC thermographs of whole milk powder (3% water content) at different heating rates (1, 5, 10 and 20°C/min respectively in green, red, blue and black curves).

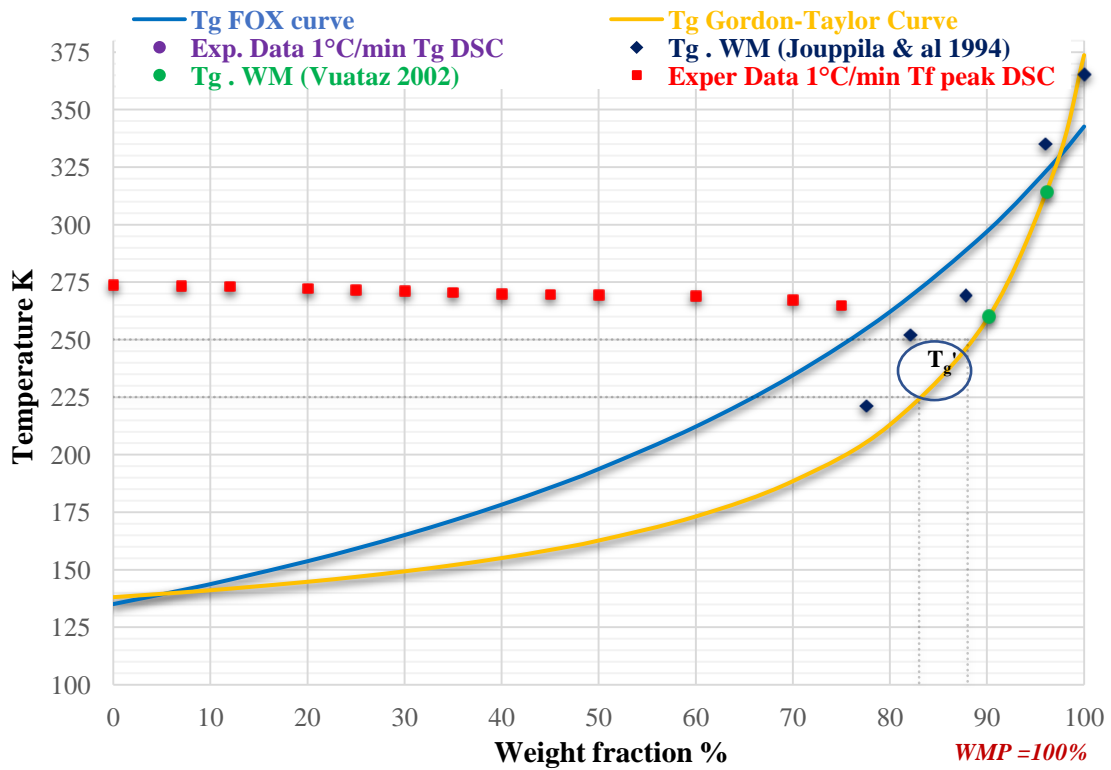
498

499

500

501

502



503

504

505

506

507

508

509

510

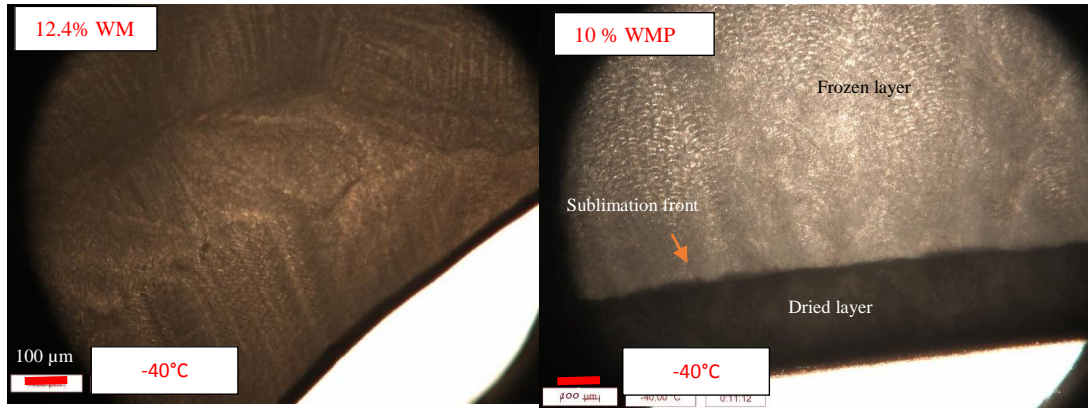
511

512

513

Figure 7. Whole Milk Powder (WMP) state diagram; Freezing temperatures measured by DSC (red square); Glass transition temperatures measured by DSC (purple circle); Glass transition temperature from bibliography (Vuataz et al. [9] (green circle), Jouppila et al. [26] (blue rhombus); Glass transition temperatures from Fox equation (blue line) and Gordon–Taylor equation (orange line). The T_g' range is between 225K and 250K.

514
515



516
517
518
519
520
521
522
523
524
525
526
527
528
529
530
531
532
533
534
535

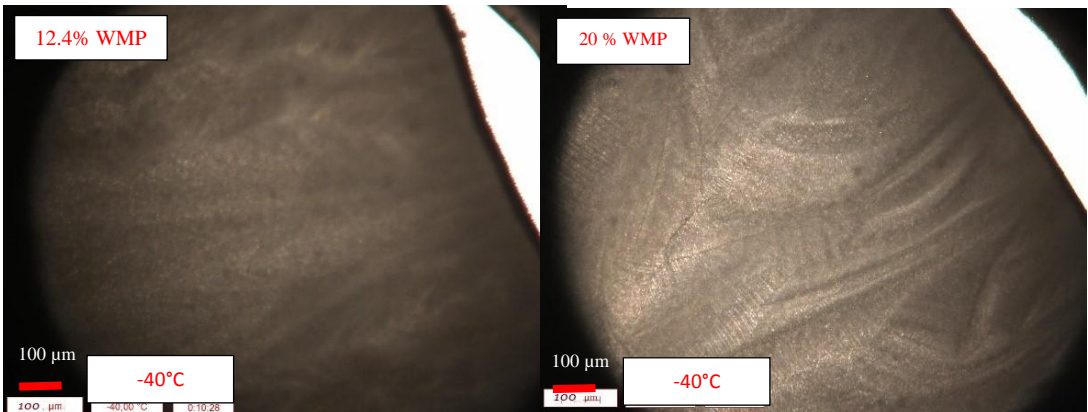
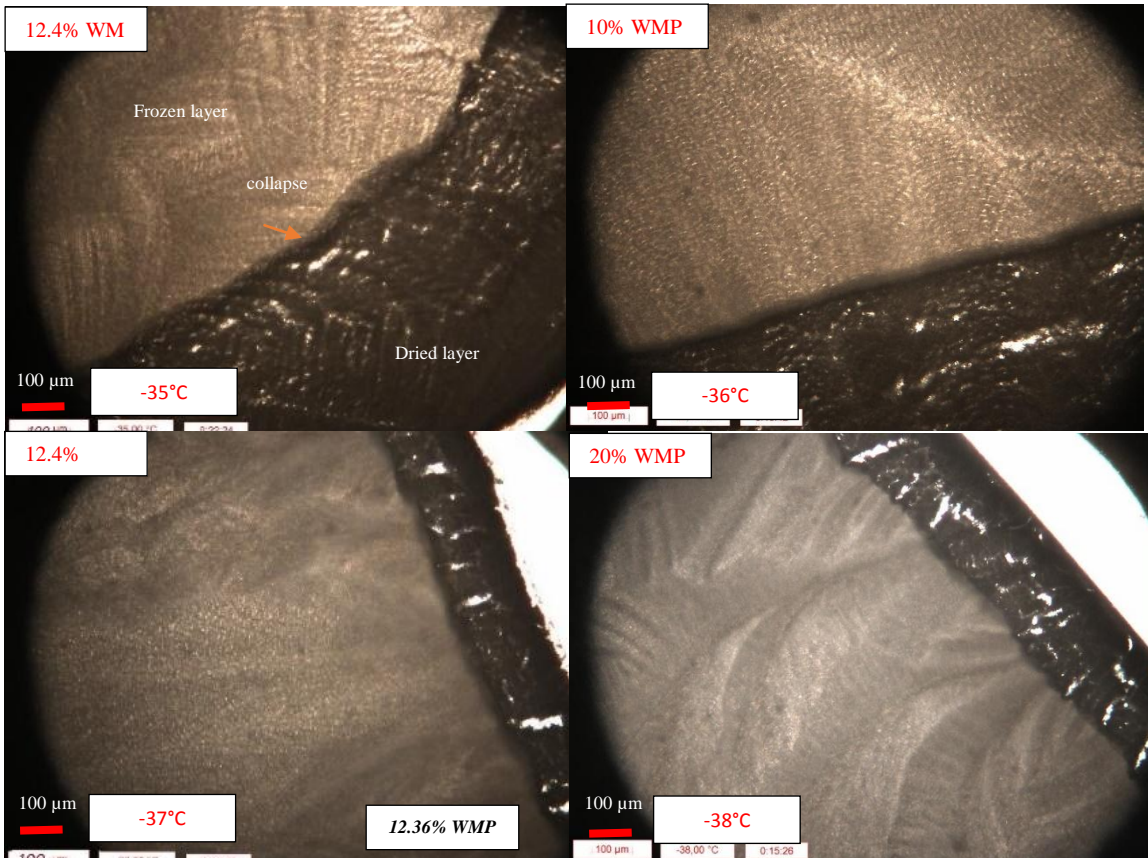


Figure 8 Microscopic observations of Whole Milk (10%, 12.4%, 20% WMP and 12.4% WM) at -40°C.



536

537

538

539

540

541

Figure 9 Collapse microscopic observations of Whole Milk (10%, 12.4%, 20% WMP and 12.4% WM).